Effective screening of localized charged perturbations in metallic nanotubes: roles of massive bands

K. Sasaki,[1] A. A. Farajian,[2] H. Mizuseki,[2] and Y. Kawazoe[2]

[1] *Department of Physics, Tohoku University, Sendai 980-8578, Japan*
[2] *Institute for Materials Research, Tohoku University, Sendai 980-8577, Japan*

(Dated: February 1, 2008)

The massive-band effects on screening behavior of metallic carbon nanotubes are theoretically investigated using two different methods; continuous and lattice quantum theories. Both approaches show screening of a localized external perturbation with an effective screening length of the order of the nanotube diameter. Calculating the nonlinear deformation of the local density of states near the charged perturbation, we show that the perturbative effects of the massive bands are effectively canceled by direct massive band interactions, such that a good agreement between the two methods can be achieved. The effective screening is important in nanoscale integration of nanotube-based electronic devices.

I. INTRODUCTION

The response of the electrons in carbon nanotubes (CNT's[1,2]) to external charged perturbations is governed by the Coulomb interaction[3,4,5]. Several aspects of the Coulomb interaction are already seen in some experiments of charging[6,7,8] and of temperature dependent resistivity[9] which are consistent with current understanding of low-energy excitations in metallic CNT's. The low-energy excitations in the metallic CNT's are theoretically modeled by *massless* bands (linear dispersion bands) with the Coulomb interaction[3,4,5]. However when we consider very localized perturbation, it is not clear if the low energy theories describe the physics correctly. Because short distance physics corresponds to high energy, *massive* bands (other sub-bands except the massless bands) would come into dynamics[10]. From the application point of view, understanding the response of CNT's to localized perturbations (e.g., individual dopant atoms) is crucial as it provides the extents of the depletion region in nanotube-based electronic devices. The importance of this issue is observed by considering the fact that in any nano-electronics application of nanotubes, different functional parts of the device, e.g., drain, source, etc., should be doped differently. In order to achieve nanoscale integration, these differently doped parts should be separated from each other by distances of the order of a few nanometers. This would not be possible if the depletion-layer length is not of the order of a few nanometers itself. In this letter, taking massive band effects explicitly into account, we focus on the screening of an external charge localized on the surface of the metallic CNT's.

It is well-known that in lower dimensional materials in which the internal electrons can move only in one or two dimensions, asymptotic behavior of the potential produced by an external charge does not become an exponential as a function of distance from the external charge. Examples of these lower dimensional materials are graphite sheet and carbon nanotubes. DiVincenzo and Mele[11] analyzed the induced charge around an external charge on the graphite sheet and found that the external charge attracts some induced charge with a characteristic length scale of the system which they called "effective screening length". A similar definition is used to describe the effective screening in metallic carbon nanotubes by Lin and Chuu[10]. In the present paper, we study the details of the pattern of induced charge around an external charge on the metallic nanotubes in order to examine the effects of massive bands on screening.

The high-energy excitations can in principle affect the screening phenomena through two different mechanisms; adding massive-fermion loop corrections to the interactions of massless bands and direct interaction of massive bands. Two methods to deal with these mechanisms are investigated. One is a quantum field theoretical method dealing with the massless bands and the one-dimensional long-range Coulomb interaction[12], with one-loop vacuum polarization correction by the massive bands. The other is a lattice model employing a fully self-consistent tight-binding approach including the interactions of massive bands[13]. It is the purpose of the present work to compare the results of these two different methods and investigate the screening nature in CNT's. Especially we shall compare the induced charge distribution around the external charge. Our results are advantageous compared to the previous works on screening in metallic nanotubes[10], as we include an effective thickness for the nanotube wall, and derive the dependence of our results on the corresponding cut-off parameter. This inclusion is crucial in reaching an agreement between the continuous and lattice results. Additionally, in our self-consistent tight-binding model there is no linear response assumption, and the deformation of local density of states (LDOS), due to the creation of localized states, are included. We also explicitly show how high-energy electron/hole excitations respond differently to the presence of a charged perturbation.

II. CONTINUOUS FIELD THEORY: ONE-LOOP MASSIVE FERMION CORRECTIONS

We begin with the quantum (continuous) field theoretical approach to the screening effect. The π-electrons in CNT's are described by two-component fermion fields ψ_{Ns} specified by the band index $N(\in \{1,\cdots\})$ and spin $s(\in \{\uparrow,\downarrow\})$. The Hamiltonian density of this system is given by $\mathcal{H} = \mathcal{H}_F + \mathcal{H}_C$ where $\mathcal{H}_F$ is the free (unperturbed) part and $\mathcal{H}_C$ is the perturbed part including the Coulomb interactions. If we include only tight-binding interactions, then $\mathcal{H}_F = \sum_{Ns} \mathcal{H}_N$ where

$$\mathcal{H}_N = \psi^\dagger_{Ns} V_\pi \begin{pmatrix} 0 & z(k^N_x, \hat{k}_y) \\ z^*(k^N_x, \hat{k}_y) & 0 \end{pmatrix} \psi_{Ns}. \qquad (1)$$

V_π is the hopping integral, $\hat{k}_y = -i\partial_y$ is the wave vector along the tubule axis, the wave vector around the circumference $ak^N_x = -\frac{2\pi}{\sqrt{3}} + \frac{2a}{d}N$ is discretized by the periodic boundary condition where d is the diameter of the CNT and a the nearest-neighbor C-C spacing. Here we take the case of metallic zigzag CNT's in which the maximum number of N is N_0 (number of hexagons along the circumference); armchair case is analyzed similarly. The function $z(k_x, k_y)$ is given by $z(k_x, k_y) = \sum_i e^{ik\cdot u_i}$. The vector u_i is a triad of vectors pointing in the direction of the nearest neighbors of a carbon site[12]. The free Hamiltonian densities $\mathcal{H}_{N_0/3}$ and $\mathcal{H}_{5N_0/3}$ describe massless fermions (electrons in massless bands) and the others are for massive fermions in the metallic zigzag CNT. The energy eigenvalues of $\mathcal{H}_N$ are given by $\pm V_\pi |z(k^N_x, k_y)|$ which reproduce a standard band structure[2]. These fermions interact with each other via the long-range Coulomb interaction:

$$\mathcal{H}_C = \frac{1}{2}\int_D J(y)V(y-y')J(y')dydy', \qquad (2)$$

where $V(y)$ is the unscreened Coulomb potential that we will specify shortly, and the internal charge density J is given by the sum of individual fermion densities: $J = \sum_{Ns} J_{Ns}$ where $J_{Ns} \equiv \psi^\dagger_{Ns}\psi_{Ns}$. Here we denote the integral region $D = [0 : L]$ and L is the system length.

Low-energy excitations in metallic CNT's are described by a field theory of four massless fermions interacting with each other and with massive fermions through the long-range Coulomb interaction. The massive fermions modify the Coulomb potential between massless fermions because of the vacuum polarization. We estimate this effect using one-loop perturbation. The modified Fourier component of the Coulomb potential is given by $\bar{\beta}_n = \frac{\beta_n}{1-\beta_n T^{ms}_n}$, where β_n is the n-th Fourier component of the unscreened Coulomb potential, $V(x) = \sum_n \beta_n e^{-i2\pi nx/L}$, and $T^{ms}_n (\le 0)$ in the denominator denotes the one-loop contribution of the *massive* fermions[14]. The unscreened Coulomb potential along the axis is[4]

$$V(x) = \frac{e^2}{4\pi\sqrt{|x|^2 + d^2 + a_z^2}} \frac{2}{\pi} K\left(\frac{d}{\sqrt{|x|^2 + d^2 + a_z^2}}\right), \qquad (3)$$

with $K(z)$ being the complete elliptic integral of the first kind and $a_z = 1.3$[Å] a cutoff length which corresponds to the Hubbard coefficient $U_H = 4V_\pi$ in the lattice model (Eq.6). The massive fermions are observed to weaken the Coulomb interaction among massless fermions as is naturally expected. Because the Coulomb potential is modified by the vacuum polarization effects, the massless fermions interact with each other via the screened Coulomb potential whose Fourier components are given by $\bar{\beta}_n$.

An external charge can be included by replacing J with $J + J^{ex}$ in the Coulomb interactions (Eq. 2), where J^{ex} is a c-number whose integral over the nanotube length is equal to the total external charge. Here we take a point external charge distribution which is modeled by $J^{ex} = \delta(x - x_0)$ where x_0 is the position of the external charge. To calculate the induced charge density, we use one-loop approximation which gives an exact result in the case of strictly linear dispersion relation[12]. In Fig. 1, the induced charge distributions around the external point charge for both the unscreened potential and the screened one are depicted. These are obtained using the following formula[14,15]:

$$\langle J(x)\rangle = \sum_{n>0} \frac{T^{ml}_n \bar{\beta}_n}{1 - T^{ml}_n \bar{\beta}_n} \frac{2}{L} \cos\left(\frac{2\pi n}{L}(x - x_0)\right), \qquad (4)$$

where T^{ml}_n is the one-loop amplitude of *massless* bands. It should be noted that the effective screening length is about the diameter of the nanotube for both cases and is not sensitive to the system length[12].

What we ignore in the above formula of induced charge density is (a) higher-order perturbative effects of massive loops on the Coulomb interaction between massless fermions, and (b) induced charge due to massive fermions (direct massive-band effect). Lin and Chuu[10] included the latter effect by adding T^{ms}_n to T^{ml}_n in the numerator of Eq.(4). This assumption, however, can only result in a linear relationship between the external and induced charges, while it is shown that linear-response theory is not sufficient at least in the case of screening in graphite[11].

III. SELF-CONSISTENT TIGHT-BINDING: NONLINEAR SCREENING

Up to now, only the massive-fermion corrections to the *massless*-band interactions, through the leading terms of vacuum polarization, were considered. We now turn to the *massive*-band effects on the screening phenomena, and investigate the influence of direct massive-band interactions. This is accomplished by using a lattice model to

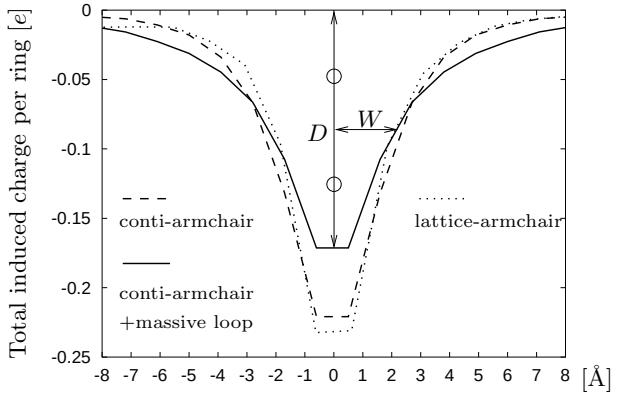

FIG. 1: Total induced charge (including spin degeneracy) around the point external charge for the (5,5) armchair tube. The dotted line is obtained from the lattice model. The solid and dashed lines are the continuous field theoretical results. The dashed one is for the calculation using unscreened Coulomb potential β_n, and the solid one is for $\bar{\beta}_n$. The screening length is about the diameter of the nanotube. Similar results are obtained for the zigzag (9,0) tube.

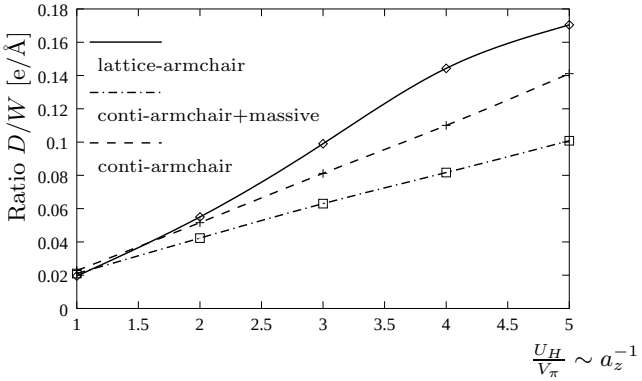

FIG. 2: The cutoff, U_H (or a_z), dependence of the ratio defined by D/W, where D is the peak of the induced charge at the position of the external charge and W is the one-half of the width at the half peak (see Fig. 1). The results show that bigger U_H (smaller a_z) gives smaller screening length. Experimentally, U_H was reported[17] to be between 2.4 and 4 V_π.

describe the nanotube. The model is essentially a tight-binding one[13] which is generalized by including long-range Coulomb interactions[16].

Within this model, the Hamiltonian of a perfect, infinite nanotube is written as $H = H_F + H_C$ with

$$H_F = \sum_{\langle i,j \rangle} V_\pi \, c_i^\dagger c_j, \tag{5}$$

$$H_C = \sum_{ij} \frac{\delta n_j}{\sqrt{r_{ij}^2 + U_H^{-2}}} \, c_i^\dagger c_i, \tag{6}$$

where U_H is the Hubbard parameter used in describing on-site interactions. Using the experimental estimation of U_H for carbon[17], we set $U_H = 4V_\pi$. U_H (corresponding to to the cut-off a_z) is the only parameter of our model and we examine the dependence of our results on this parameter, by considering several cases of U_H (or a_z). In Eq.6, $\delta n_i = n_i - n_i^0$ is the change in the self-consistent and screened occupation number n_i at site i, as compared to the occupation imposed by external perturbation, n_i^0. Therefore, δn_i would be the induced charge at site i, in response to the external perturbation. We are concerned with localized perturbation, which is modeled by modifying n_i^0 as $n_i^0 \to n_i^0 + n_i^{ex}$.

We distinguish three different parts in the infinite nanotube: An unperturbed semi-infinite part to the left, a perturbed finite part in the middle, and an unperturbed semi-infinite part to the right. In the unperturbed parts, $n_i^0 = 0.5$ (excluding the spin degeneracy) and $\delta n_i = 0$. This implies that the length of the perturbed finite part, for which δn_i's are assumed to be nonzero, is chosen to be long enough such that the external perturbation is fully screened within this part of the nanotube. For concreteness, we assume that the localized external perturbation only modifies the sites of the two carbon rings of the nanotube by adding n_i^{ex}'s to the corresponding n_i^0's. (A ring consists of all the carbon atoms with the same longitudinal coordinate along the nanotube axis.) The two rings with nonzero n_i^{ex}'s are assumed to be at the middle of the perturbed finite part of the nanotube, which, in turn, is taken to consist of 16 carbon rings. This number of carbon rings has proven [13] to be long enough in order to derive the converged induced charges, as increasing the number of rings has had no effect on the self-consistent occupations.

The self-consistent procedure of calculating the induced charges δn_i's proceeds as follows [13]: Starting with an initial guess of zero δn_i's in the Hamiltonian Eq.6, the surface Green's functions, G_L and G_R, of the two semi-infinite unperturbed parts to the left and right of the perturbed region, are calculated[18]. These surface Green's functions are then attached to the Green's function of the perturbed middle part, $G_P = (z - H_P)^{-1}$, where z is the complex energy and H_P is the Hamiltonian of the perturbed region, in order to obtain the total Green's function of the system, G_T, projected onto the perturbed region[19,20,21,22,23,24]:

$$G_T = (G_P^{-1} - V_{PL} G_L V_{LP} - V_{PR} G_R V_{RP})^{-1}. \tag{7}$$

Here, V matrices indicate the coupling between the perturbed region and the first unit cells of the unperturbed parts to the left and right. Using Eq.7, the LDOS at site i in the perturbed region, $g_i(E) = [G_T(i,i) - G_T^*(i,i)]/2\pi$, is derived. The induced charges can be obtained through integrating $g_i(E)$'s. δn_i's are then used to initialize the Hamiltonian for another round of δn_i's calculation. This procedure is continued until the induced charges are determined self-consistency. Throughout the self-consistent calculation, the chemical potential of the system is assumed to be that of the unperturbed nanotube, as after

screening the whole system would be in thermal equilibrium and would have a unique chemical potential. Furthermore, the external perturbation being localized and finite, the unique chemical potential would be that of the unperturbed semi-infinite parts of the nanotube, which act like reservoirs attached to the perturbed finite part.

As specific examples, an armchair (5,5) and a zigzag (9,0) nanotube are considered, whose diameters are 6.78 and 7.04 [Å]. The external perturbation of the middle two rings of the perturbed part of these tubes are defined as $n_i^{ex} = 0.0250$ and $n_i^{ex} = 0.0278$, for the armchair and zigzag tubes, respectively. This external perturbation amounts to adding a total charge of $1.0e$ to the middle two rings for both the armchair and the zigzag tubes.

Comparing the self-consistent procedure used in the tight-binding model of the present work with the tight-binding approach of Lin and Chuu[10], we notice that in our model there is no restriction on the shape of the LDOS within the perturbed region. In fact, the very shape of the LDOS is calculated self-consistently, as described above. Lin and Chuu's approach, however, assumes fixed energy dispersion relations for the whole nanotube, and restricts the modifications due to the charged perturbation to the linear response theory via dielectric constant and response function. Our model is therefore advantageous, as it properly takes into account the nonlinear effects of the localized states which are produced within the perturbed region. This is explicitly observed from the LDOS curves in the perturbed region, as will be shown shortly.

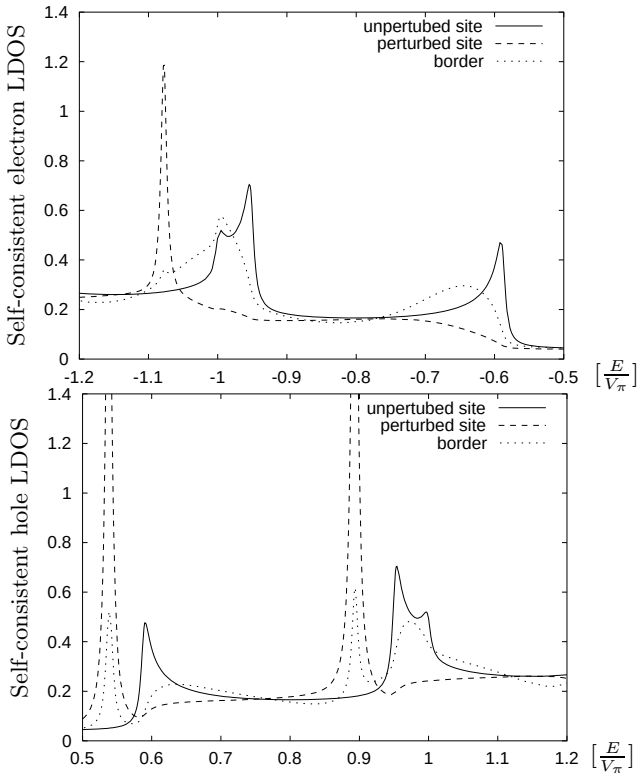

FIG. 3: Self-consistent electron (top) and hole (bottom) LDOS. Fermi energy is located at zero.

IV. COMPARISON AND DISCUSSION

The resultant induced charges for the (5,5) armchair tube are depicted in Fig. 1. It is observed that the effective screening length is of the order of the nanotube diameter, in all the different calculations. The length also depends on the cutoff a_z or the Hubbard coefficient U_H. The cutoff dependence of induced charge pattern is plotted for several U_H values in Fig. 2. The main features of the induced charge pattern are observed to hold for the whole range of experimentally reported U_H[17]. From Fig. 1 we further see that the induced charges obtained by including only the massless bands in the continuous field-theoretical calculation are in qualitative agreement with the results of lattice calculation, which, in addition to the massless bands, includes the effects of direct massive bands interactions. Interestingly, including the massive-loop corrections to massless bands interactions does not result in better agreement with the results of lattice model. This suggests that, within the continuous model, the massive-loop corrections to the massless band interactions somehow cancel the effects of direct massive band interactions, such that the results of a calculation based only on massless bands turn out to be in agreement with the results of the lattice model. In other words, in the continuous approach, the induced charge density is given by the sum of two densities as $\langle J\rangle = \langle J_{\rm massless}\rangle + \langle J_{\rm massive}\rangle$ where $\langle J_{\rm massless}\rangle$ is defined in Eq.4. $\langle J_{\rm massive}\rangle$ is an induced charge density due to massive bands themselves, and is what we have ignored. Perturbative inclusion of massive bands reduces the peak of the former charge density and results in a more appreciable difference with the lattice results. Considering overall agreement of the lattice results and continuous field theoretical results based on the massless bands, it is natural to expect that $\langle J_{\rm massive}\rangle$ partially cancels the perturbative effects of the massive bands on the massless bands interaction, such that the net induced charge density is basically decided by the massless bands.

In addition to the calculations for the armchair tube, we have performed similar calculations on the (9,0) zigzag tube. The results of the continuous model[12] show the same features, as those of the armchair one, when compared to the results of lattice model. This indicates that the agreement between the continuous massless results and lattice results is not accidental. It is remarkable that in both the continuous and lattice calculations the peak value of the induced charge shows a reduction of $\sim 15\%$, when one compares zigzag results with armchair results.

In order to see the LDOS deformation, the creation of localized states within the perturbed region, and the effects of massive bands more clearly, we show the self-consistent LDOS's for a typical unperturbed site (solid line), a site located at one of the rings perturbed exter-

nally (dashed line), and a site, of the perturbed portion of the nanotube, located at the furthest ring relative to the middle two rings (dotted line) in Fig. 3. The latter site indicates the border between the perturbed finite part of the tube and one of the unperturbed semi-infinite parts. In Fig. 3, enlarged typical regions of the electron (hole) LDOS's are depicted. It is clearly seen that the densities of massive states in the perturbed region are different from the corresponding densities of the unperturbed region. However, as one expects, the difference is much more pronounced near the location of external perturbation than far from it. This is indeed an indication of localized-states creation. The border LDOS shows how the extremely perturbed LDOS near the external perturbation transforms rather smoothly, as one moves toward the border of the perturbed region, into the unperturbed LDOS. Another very interesting feature is the difference in the behavior of the electron states as compared to the hole states. For the external perturbation mentioned above, namely *addition* of one extra electron to the middle two rings, it is seen that the hole states tend to accumulate at lower energies, while the electron states are pushed toward higher energies. This indicates the decisive effect of the Coulomb interactions among the massive fermion- (both electron- and hole-) states. One should notice that, due to the rotational symmetry selection rule [13], the electron/hole states belonging to a certain band are not allowed to jump over to another band with higher/lower energy. But *within each band* the electron states tend to concentrate at higher energies, and the hole states tend to concentrate at lower energies. This is indeed the reason for the enhanced/decreased densities at band edges.

V. CONCLUSIONS

In summary, we have analyzed the charge screening in metallic nanotubes using two different methods, including explicitly the massive bands effects, based on lattice and continuous models. In both methods, a localized external charge is shown to be screened with an effective screening length about the diameter of the tube. The local density of states, calculated by the lattice model, indicates the formation of the localized states within the perturbed region, and shows that the massive bands are strongly affected by the external charge. As for the continuous field theoretical model, we have included the massive bands one-loop corrections in massless bands interactions. Although non-perturbative effects of massive bands were not considered, the results show basically the same pattern as that of the lattice model results. This shows that the perturbative corrections of massive bands are efficiently canceled by the induced charge due to massive bands themselves. The short effective screening length reported here makes it possible, at least theoretically, to achieve nanoscale integration of nanotube-based electronic devices.

Acknowledgments

A.A.F., H.M. and Y.K. are supported by the Special Coordination Funds of the Ministry of Education, Culture, Sports, Science and Technology of the Japanese government.

[1] S. Iijima, Nature **354**, 56 (1991).
[2] R. Saito, G. Dresselhaus, and M.S. Dresselhaus, *Physical Properties of Carbon Nanotubes*, (Imperial College Press, London, 1998).
[3] C. Kane, L. Balents, and M.P.A. Fisher, Phys. Rev. Lett. **79**, 5086 (1997).
[4] R. Egger and A.O. Gogolin, Phys. Rev. Lett. **79**, 5082 (1997); Eur. Phys. J. B **3**, 281 (1998).
[5] H. Yoshioka and A.A. Odintsov, Phys. Rev. Lett. **82**, 374 (1999).
[6] S.J. Tans, M.H. Devoret, H. Dai, A. Thess, R.E. Smalley, L.J. Geerligs, and C. Dekker, Nature **386**, 474 (1997).
[7] S.J. Tans, M.H. Devoret, R.J.A. Groeneveld, and C. Dekker, Nature **394**, 761 (1998).
[8] H.W.Ch. Postma, Z. Yao, and C. Dekker, J. Low. Temp. Phys. **118**, 495 (2000).
[9] M. Bockrath, D.H. Cobden, J. Lu, A.G. Rinzler, R.E. Smalley, L. Balents, and P.L. McEuen, Nature **397**, 598 (1999); H.W.Ch. Postoma, T. Teepen, Z. Yao, M. Crifoni, and C. Dekker, Science **293**, 76 (2001).
[10] M.F. Lin and D.S. Chuu, Phys. Rev. B **56**, 4996 (1997).
[11] D.P. DiVincenzo and E.J. Mele, Phys. Rev. B **29**, 1685 (1984).
[12] K. Sasaki, Phys. Rev. B **65**, 155429 (2002); *ibid.* **65**, 195412 (2002).
[13] A.A. Farajian, K. Esfarjani, and Y. Kawazoe, Phys. Rev. Lett. **82**, 5084 (1999); A.A. Farajian, K. Esfarjani, and M. Mikami, Phys. Rev. B **65**, 165415 (2002).
[14] K. Sasaki, A.A. Farajian, H. Mizuseki, and Y. Kawazoe, arXiv:cond-mat/0207149.
[15] We set n equal to $L/\sqrt{3}a$ for the armchair CNT. This cutoff may cause an oscillatory pattern[12] of the induced charge density for the Coulomb interaction with shorter cutoff length a_z.
[16] K. Harigaya and S. Abe, Phys. Rev. B **49**, 16746 (1994).
[17] R.G. Pearson, Inorg. Chem. **27**, 734 (1988).
[18] M.P. López Sancho, J.M. López Sancho, and J. Rubio, J. Phys. F: Met. Phys. **15**, 851 (1985).
[19] P.A. Lee and D.S. Fisher, Phys. Rev. Lett. **47**, 882 (1981).
[20] A. MacKinnon, Z. Phys. B: Condens. Matter **59**, 385 (1985).
[21] M.C. Munoz, V.R. Velasco, and F. Garcia-Moliner, Prog. Surf. Sci. **26**, 117 (1987).
[22] F. Garcia-Moliner and V.R. Velasco, *Theory of single and multiple interfaces*, (World Scientific, Singapore, 1992).
[23] S. Datta, *Electronic Transport in Mesoscopic Systems*,

(Cambridge University Press, Cambridge, UK, 1995).
[24] L. Chico, L.X. Benedict, S.G. Louie, and M.L. Cohen, Phys. Rev. B **54**, 2600 (1996).